ISSN 1063-7761, Journal of Experimental and Theoretical Physics, 2008, Vol. 107, No. 4, pp. 603–611. © Pleiades Publishing, Inc., 2008.
Original Russian Text © V.A. Ignatchenko, Yu.I. Mankov, D.S. Tsikalov, 2008, published in Zhurnal Éksperimental'noĭ i Teoreticheskoĭ Fiziki, 2008, Vol. 134, No. 4, pp. 706–715.

ORDER, DISORDER, AND PHASE TRANSITION IN CONDENSED SYSTEMS

High-Frequency Susceptibility of a Superlattice with 2D Inhomogeneities

V. A. Ignatchenko[a], Yu. I. Mankov[a,b], and D. S. Tsikalov[b]

[a] *L.V. Kirenskii Institute of Physics, Russian Academy of Sciences, Siberian Branch, Krasnoyarsk, 660036 Russia*

[b] *Siberian Federal University, Krasnoyarsk, 660062 Russia*

e-mail: mankov@iph.krasn.ru

Received April 7, 2008

Abstract—We investigate the high-frequency susceptibility (Green function) of an initially sinusoidal 1D superlattice with 2D phase inhomogeneities that model the deformations of the interfaces between the superlattice layers. For waves propagating along the superlattice axis (the geometry of a photon or magnon crystal), we have found a peculiar behavior of the imaginary part of the Green function that consists in a significant difference between the peaks corresponding to the edges of the band gap in the wave spectrum. The peak corresponding to the lower-frequency band edge remains essentially unchanged as the root-mean-square fluctuation of the 2D inhomogeneities γ_2 increases, while the peak corresponding to the higher-frequency band edge broaden and decreases sharply in height until its complete disappearance with increasing γ_2. This behavior of the peaks corresponds to a band gap closure mechanism that differs from the traditional one characteristic of 1D and 3D inhomogeneities. These effects can be explained by a peculiarity of the energy conservation laws for the incident and scattered waves for 2D inhomogeneities in a 1D superlattice.

PACS numbers: 68.65.-k, 75.30.Ds, 68.65.Cd

DOI: 10.1134/S1063776108100075

1. INTRODUCTION

At present, multilayered film structures (1D superlattices) that consist of periodically alternating layers of two or more materials with different physical properties are being investigated extensively. In particular, photon and magnon crystals that have received much attention belong to such structures. The spectrum of waves of any nature in periodic systems is known to have a band structure characterized by the reciprocal lattice vector $\mathbf{q}$ ($|\mathbf{q}| \equiv q = 2\pi/l$, where l is the 1D superlattice period). The degeneracy is removed and band gaps $\Delta\omega_n$ appear at the edge of the Brillouin zones in a superlattice at $k = nq/2$. The gap width is determined by the change in the physical parameters of the neighboring layers and by the band number n. In actual materials, an ideal periodicity in the arrangement of layers can be maintained only approximately. There are always random deviations from periodicity due to natural or technological factors; the purposeful formation of a particular aperiodicity is also possible. This has stimulated the appearance of theoretical works in which the transition from ideally periodic superlattices to partially stochastized ones is studied.

Several theoretical methods have been developed to date to investigate the spectral properties of such superlattices: the introduction of a 1D random phase [1, 2]; modeling the disorder in the arrangement of layers of two different materials [3–9]; the numerical simulation of random deviations of the interfaces between layers from their initial periodic arrangement [10–12]; postulating the form of the correlation function for a superlattice with inhomogeneities [13, 14]; the application of geometrical optics approximations [15]; and the development of a dynamical theory of composite elastic media [16].

In [17–23], the method of averaged Green functions was used to describe the spectral properties of superlattices. The only characteristic describing a random medium that appears in the expression for the averaged Green function is the correlation function $K(\mathbf{r})$, which depends on the distance $\mathbf{r}$ between two points of the medium: $\mathbf{r} = \mathbf{x} - \mathbf{x}'$. Therefore, the first part of the problem is reduced to finding the function $K(\mathbf{r})$ for a superlattice with particular inhomogeneities and its second part consists in extracting the spectral characteristics from the expression for the Green function containing this correlation function by standard approximate methods. The model of a random phase that was assumed to be a function of all three coordinates with an arbitrary correlation length was used to describe the inhomogeneities of the geometric structure of an initial sinusoidal superlattice. A random space modulation (RSM) method [17] was developed to find the correlation function $K(\mathbf{r})$ of a superlattice. This method is a

generalization of the well-known method of determining the time correlation function for the random frequency (phase) modulation of a radio signal [24, 25] to the case of a space (generally 3D) modulation of the superlattice period. The advantage of this method is that the form of the correlation function for a superlattice is not postulated but is derived from the most general assumptions about the pattern of random space modulation of the superlattice period. This function was shown to generally have a complex form that depends significantly on the size of the inhomogeneities, the structure of the interfaces between layers, etc.

The spectrum of waves, their damping, and the high-frequency susceptibility of an initially sinusoidal superlattice that contained 1D phase inhomogeneities modeling the random displacements of the interfaces between the superlattice layers from their initial periodic arrangement and 3D isotropic phase inhomogeneities modeling the random deformations of these interfaces were investigated in [17–23]. The influence of the simultaneous presence of 1D and 3D inhomogeneities on the spectral characteristics was also investigated both in the absence [20] and in the presence [22, 23] of cross- correlations between them.

Inhomogeneous deformations of the interfaces between layers should generally be modeled by anisotropic 3D correlation functions with different correlation lengths: $\tilde{r}_{||}$ along the superlattice z axis and $\tilde{r}_{\perp}$ in the xy plane of the superlattice layers. A wide variety of relations between these correlation lengths can be encountered in practice. The relation between the correlation length $\tilde{r}_{||}$ and the mean superlattice layer thickness $l/2$ can also play a significant role in this case. If $\tilde{r}_{||} \ll l/2$, then the deformations of the neighboring layers are virtually independent. If $\tilde{r}_{||} \gtrsim l/2$, then the deformations on the neighboring layers are correlated. The extreme case of large correlation lengths $\tilde{r}_{||}$ where both inequalities hold, $\tilde{r}_{||} \gg l/2$ and $\tilde{r}_{||} \cong \tilde{r}_{\perp}$, corresponds to complete identity of the inhomogeneities at all interfaces between the superlattice layers. In this extreme case, an anisotropic 3D correlation function turns into a 2D one.

In practice, such a situation can take place, for example, when the inhomogeneities of the superlattice layer surfaces result from an inhomogeneous deformation of the substrate on which these layers are deposited. In this case, the random (in the xy plane) deformations can be repeated almost in phase on the surface of each new deposited layer and the superlattice will be roughly described by a 2D correlation function with a finite correlation length in the xy plane and an infinite one along the z axis.

The modification of the dispersion law and the damping of a sinusoidal superlattice due to 2D inhomogeneities were briefly considered in [17]. In this case, in contrast to 1D and 3D inhomogeneities, the damping due to 2D inhomogeneities was shown to arise only on one branch in the spectrum located above the gap at the boundary of the Brillouin zone, while the frequency of the lower branch remains real. In this paper, we investigate the high-frequency susceptibility (Green function) of a sinusoidal superlattice with 2D inhomogeneities and discuss the physical mechanism that leads to an asymmetry in the influence of such inhomogeneities on the lower and upper branches of the wave spectrum.

2. THE MODEL AND CORRELATION FUNCTION OF A SUPERLATTICE

Recall briefly the main features of the model and method used in [17–23]. The superlattice is characterized by the dependence of some material parameter A on the spatial coordinates $\mathbf{x} = \{x, y, z\}$. The parameter $A(\mathbf{x})$ can vary in physical nature. This parameter can be the density of the material or the force constant for an elastic medium, the magnetic anisotropy, magnetization, or exchange for a magnetic system, etc. We will represent $A(\mathbf{x})$ as

$$A(\mathbf{x}) = A + \Delta A \rho(\mathbf{x}), \tag{1}$$

where A is the mean value of the parameter, ΔA is its root-mean-square (rms) deviation, and $\rho(\mathbf{x})$ is a centered ($\langle \rho(\mathbf{x}) \rangle = 0$) and normalized ($\langle \rho^2(\mathbf{x}) \rangle = 1$) function. The function $\rho(\mathbf{x})$ describes both the periodic dependence of the parameter along the superlattice z axis and the random space modulation of this parameter, which generally can be a function of all three coordinates: $\mathbf{x} = \{x, y, z\}$. The angular brackets denote averaging over an ensemble of random realizations of $\rho(\mathbf{x})$.

We consider a superlattice with a sinusoidal dependence of the material parameter on the z coordinate in the initial state when there are no random inhomogeneities. As in [17], we will represent the function $\rho(\mathbf{x})$ as

$$\rho(\mathbf{x}) = \sqrt{2}\cos\{q[z - u_d(\mathbf{x})] + \psi\}, \tag{2}$$

where $d = 1, 2, 3$ is the dimension of the inhomogeneities. The sinusoidal superlattice may be considered as a special case of a multilayered structure with very smooth interfaces between the layers. In this case, the positive and negative regions of $\rho(\mathbf{x})$ along the superlattice z axis correspond to the alternating layers of such a multilayered structure and the zero points of $\rho(\mathbf{x})$ correspond to the interfaces between the superlattice layers. In this interpretation, depending on the value of d, the function $u_d(\mathbf{x})$ models the random displacements ($d = 1$) or the random deformations ($d = 3$ or 2) of these interfaces. The coordinate-independent phase ψ is distributed uniformly in the interval $(-\pi, \pi)$.

The static and dynamic properties of randomly inhomogeneous materials are determined by the stochastic properties of their inhomogeneities described by the correlation function. Let us calculate it for the superlattice under consideration.

The correlation function $K(\mathbf{r})$ depends only on the coordinate difference $\mathbf{r} = \mathbf{x} - \mathbf{x}'$ and is defined by

$$K(\mathbf{r}) = \langle \rho(\mathbf{x})\rho(\mathbf{x}+\mathbf{r})\rangle_{\psi\chi}. \quad (3)$$

Here, the averaging is performed both over the random phase ψ and over the random function χ, where

$$\chi(\mathbf{x}, \mathbf{r}) = q[u_d(\mathbf{x}+\mathbf{r}) - u_d(\mathbf{x})]. \quad (4)$$

Under the assumption of a Gaussian distribution of χ, a general expression was derived for $K(\mathbf{r})$ in the form [17]

$$K(\mathbf{r}) = \cos(qr_z)K_d(\mathbf{r}), \quad (5)$$

where the decreasing part of the correlation function $K_d(\mathbf{r})$ is defined by

$$K_d(\mathbf{r}) = \exp\left[-\frac{1}{2}Q_d(\mathbf{r})\right]. \quad (6)$$

Here,

$$Q_d(\mathbf{r}) = q^2\langle[u_d(\mathbf{x}+\mathbf{r}) - u_d(\mathbf{x})]^2\rangle$$

is the dimensionless superlattice structure function that can be represented as

$$Q_d(\mathbf{r}) = 2q^2\int\frac{d\mathbf{k}}{k^2}S_\varphi(\mathbf{k})(1 - \cos(\mathbf{k}\cdot\mathbf{r})), \quad (7)$$

where $S_\varphi(\mathbf{k})$ is the spectral density of the correlation function $K_\varphi(\mathbf{r})$ that describes the stochastic properties of the gradient of the modulating function $u_d(\mathbf{x})$ (recall that the stochastic properties of $u_d(\mathbf{x})$ cannot be described by a correlation function that depends only on the coordinate difference $\mathbf{x} - \mathbf{x}'$, since $u_d(\mathbf{x})$ is not a homogeneous random function):

$$S_\varphi(\mathbf{k}) = \frac{1}{(2\pi)^3}\int K_\varphi(\mathbf{r})e^{-i\mathbf{k}\cdot\mathbf{r}}d\mathbf{r}. \quad (8)$$

The correlation function $K_\varphi(\mathbf{r})$ in this expression can be chosen from the most general ideas of the pattern of random modulation $u_d(\mathbf{x})$. For 2D inhomogeneities, the random modulation u_2 depends only on the vectors

$$\mathbf{x}_\perp = \{x, y\}, \quad \mathbf{r}_\perp = \{r_x, r_y\},$$

that lies in the xy plane. To model the 2D deformations of the interfaces in the superlattice, we will choose the correlation function that describes isotropic (in the xy plane), exponentially decreasing correlations:

$$K_\varphi(\mathbf{r}) = \sigma_2^2\exp(-k_2r_\perp), \quad (9)$$

where σ_2 is the rms fluctuation of the gradient of the random function $u_2(\mathbf{x}_\perp)$, k_2 is the correlation wave number of the 2D inhomogeneities ($k_2^{-1} = \tilde{r}_\perp$ is the correlation length), and $r_\perp = |\mathbf{r}_\perp|$. The spectral density $S_\varphi(\mathbf{k})$ defined by Eq. (8) is then

$$S_\varphi(\mathbf{k}) = \frac{\sigma_2^2}{2\pi}\delta(k_z)\frac{k_2}{(k_2^2 + k_x^2 + k_y^2)^{3/2}}. \quad (10)$$

Substituting (10) into (7) and integrating yields

$$Q_2(\mathbf{r}) = 4\gamma_2^2\{E_1(k_2r_\perp) + \ln(k_2r_\perp C) + \exp(-k_2r_\perp) - 1\}. \quad (11)$$

Here, $C \approx 1.78$ is the Euler constant,

$$E_1(z) = \int_z^\infty\frac{e^{-t}}{t}dt$$

is the integral exponential function, and the parameter $\gamma_2 = q\sigma_2/\sqrt{2}\,k_2$ defines the rms fluctuations of the function $u_2(\mathbf{x}_\perp)$. In the extreme cases of large and small $r_\perp$, Eq. (11) takes the form

$$Q_2(\mathbf{r}) = \gamma_2^2\begin{cases}k_2^2r_\perp^2, & k_2r_\perp \ll 1\\ 4\ln(k_2r_\perp C/e), & k_2r_\perp \gg 1,\end{cases} \quad (12)$$

where e is the base of the natural logarithm.

Recall that a Gaussian modeling correlation function was used in [17] when the dispersion law and damping of waves in a superlattice with 2D phase inhomogeneities were investigated,

$$K_\varphi(\mathbf{r}) = \sigma_2^2\exp\left(-\frac{1}{2}k_2^2r_\perp^2\right). \quad (13)$$

Accordingly, an expression differing from (11) was derived for $Q_2(\mathbf{r})$. However, in the extreme cases for both $k_2r_\perp \ll 1$ and $k_2r_\perp \gg 1$, this expression matches Eq. (12). This confirms the general proposition that the correlation function $K(\mathbf{r})$ of a superlattice is asymptotically independent of the form of the modeling function $K_\varphi(r)$, which was established previously for 1D and 3D inhomogeneities [17]. At the same time, the asymptotics of the correlation function $K(\mathbf{r})$ for the superlattice differ significantly for 1D, 2D, and 3D phase inhomogeneities.

Substituting Eq. (11) for $Q_2(\mathbf{r})$ into Eq. (6) yields an excessively cumbersome expression for the correlation function $K(\mathbf{r})$. Therefore, we approximated the decreasing part of the correlation function $K_2(\mathbf{r})$ by the expression

$$K_2(\mathbf{r}) = \left(1 + \frac{C^2}{e^2}k_2^2r_\perp^2\right)^{-\gamma_2^2}. \quad (14)$$

Figure 1 shows the decreasing parts of the exact correlation function (6) with $Q_2(\mathbf{r})$ in form (11) and the approximating function $K_2(\mathbf{r})$ in form (14) for $\gamma_2^2 = 0.3$ and 1.0. We see that the model correlation function

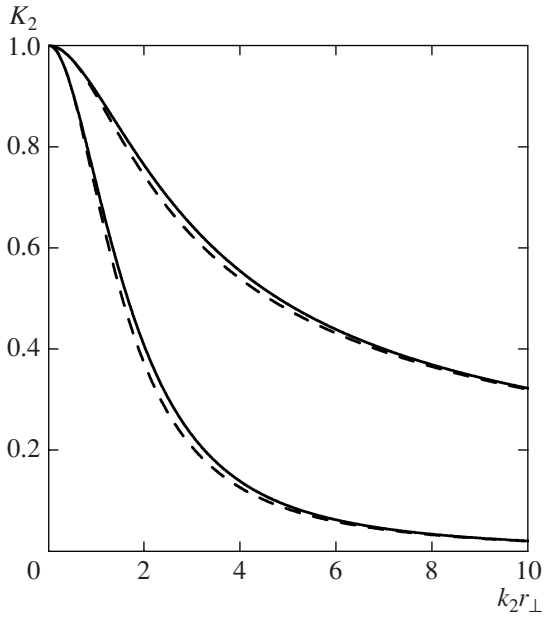

Fig. 1. Decreasing part of the correlation function for a superlattice with 2D inhomogeneities for $\gamma_2^2 = 0.3$ (the upper pair of curves) and $\gamma_2^2 = 1.0$ (the lower pair of curves). The solid and dashed curves correspond to Eq. (6) with $Q_2(\mathbf{r})$ in form (11) and the approximating correlation function (14), respectively.

describes well the exact one in the entire $r_\perp$ range and has asymptotics coincident with that of the exact function for both $k_2 r_\perp \ll 1$ and $k_2 r_\perp \gg 1$. The latter is the main requirement in choosing the approximating correlation function, since, as was shown previously [20–23] (for both 1D and 3D inhomogeneities and for their mixture), the spectral properties of the waves are determined mainly by the asymptotic form of the correlation function for the inhomogeneities when $r \longrightarrow \infty$.

3. THE HIGH-FREQUENCY SUSCEPTIBILITY OF A SUPERLATTICE

The wave equation for the time Fourier transform in a superlattice can be represented as

$$\nabla^2 m + \left[\nu - \frac{\Lambda}{\sqrt{2}}\rho(\mathbf{x})\right]m = 0, \tag{15}$$

where the function $m = m(\mathbf{x}, \omega)$ and the parameters ν and Λ are different for waves of different nature. For spin waves, Eq. (15) corresponds to a ferromagnetic superlattice with a nonuniform magnetic anisotropy parameter $\beta(\mathbf{x})$ ($A = \beta$ and $\Delta A = \Delta\beta$ in Eq. (1)) in a situation where the directions of the external magnetic field $\mathbf{H}$, the constant magnetization component $\mathbf{M}_0$, and the magnetic anisotropy axis coincide with the direction of the superlattice z axis. In this case, $m = M_x + iM_y$, $\nu = (\omega - \omega_0)/\alpha g M_0$, and $\Lambda = \sqrt{2}\,\Delta\beta/\alpha$, where ω is the frequency, $\omega_0 = g[H + (\beta - 4\pi)M_0]$ is the frequency of a uniform ferromagnetic resonance, g is the gyromagnetic ratio, and α is the exchange constant. For elastic waves in the scalar approximation in a superlattice with a nonuniform density of the medium $p(\mathbf{x})$ ($A = p$ and $\Delta A = \Delta p$), we have $\nu = (\omega/s)^2$ and $\Lambda = \sqrt{2}\,\omega^2(\Delta p)/ps^2$, where s is the speed of the elastic waves. For electromagnetic waves in the same approximation in a medium with a nonuniform permittivity $\varepsilon(\mathbf{x})$ ($A = \varepsilon$ and $\Delta A = \Delta\varepsilon$), we have $\nu = \varepsilon(\omega/c)^2$ and $\Lambda = \sqrt{2}\,\omega^2(\Delta\varepsilon)/\varepsilon c^2$, where c is the speed of light.

The Fourier transform of the averaged Green function for Eq. (15) is

$$G(\nu, \mathbf{k}) = \frac{1}{\nu - k^2 - M(\nu, \mathbf{k})}, \tag{16}$$

where $M(\nu, \mathbf{k})$ is a classical analogue of the mass operator that can be represented in Bourret's approximation [26] as [19]

$$M(\nu, \mathbf{k}) = -\frac{\Lambda^2}{8\pi}\int \frac{K(\mathbf{r})}{|\mathbf{r}|} \times \exp[-i(\mathbf{k}\cdot\mathbf{r} + \sqrt{\nu}|\mathbf{r}|)]d\mathbf{r}. \tag{17}$$

Let us calculate the Green function (16) for the waves in a superlattice with 2D inhomogeneities. Passing to a spherical coordinate system with the polar axis along the z axis ($\mathbf{k} \parallel z$) in Eq. (17) for the mass operator and integrating over the azimuth angle, we obtain

$$M(\nu, \mathbf{k}) = -\frac{\Lambda^2}{2}\int_0^\infty dr r \exp(-i\sqrt{\nu}r) \times \int_0^1 dc \frac{\cos(qrc)\cos(krc)}{\left[1 + \frac{C^2}{e^2}k_2^2 r^2(1 - c^2)\right]^{\gamma_2^2}}, \tag{18}$$

where $c = \cos\vartheta$, ϑ is the polar angle.

Here, we investigate the high-frequency susceptibility at the edge of the first Brillouin zone at $k = k_r \equiv q/2$. After the integration over r in Eq. (18), substituting the derived expression into the Green function (16) and introducing dimensionless quantities, we obtain in the two-wave approximation

$$\Lambda G(\nu) = \left\{X + \frac{\nu_r}{2\Lambda\eta_2^2}\left(\frac{e}{C}\right)^{2\gamma_2^2} \times \int_0^1 \frac{dc}{(1 - c^2)^{\gamma_2^2}} J(c, X)\right\}^{-1}, \tag{19}$$

where $X = (\nu - \nu_r)/\Lambda$, $\nu_r = k_r^2$, $\eta_2 = 2k_2 k_r/\Lambda$:

$$J(c, X) = -2^{-1/2-\gamma_2^2}\sqrt{\pi}\Gamma(1-\gamma_2^2) \times\left(\frac{e^2}{C^2(1-c^2)}\right)^{1-\gamma_2^2}\left[\frac{2^{-1/2+\gamma_2^2}}{\sqrt{\pi}\Gamma(2-\gamma_2^2)} - \frac{\mathbf{H}_{3/2-\gamma_2^2}(iw)}{(iw)^{1/2-\gamma_2^2}} + \frac{Y_{3/2-\gamma_2^2}(iw)}{(iw)^{1/2-\gamma_2^2}}\right]. \quad (20)$$

Here, we denote

$$w = \frac{e}{\eta_2 C\sqrt{1-c^2}}\left[X + \frac{2\nu_r}{\Lambda}(1-c)\right], \quad (21)$$

$\mathbf{H}_\alpha(z)$, $Y_\alpha(z)$, and $\Gamma(z)$ are the Struve, Neumann, and gamma functions, respectively. However, Eq. (20) is valid at $\gamma_2^2 \neq n$, where n is an integer. At $\gamma_2^2 = n$, simpler expressions appear in Eq. (19) instead of the function $J(c, X)$. Thus, for example, at $\gamma_2^2 = 1$, we should right the following function under the integral in (19):

$$J_1(c, X) = \frac{1}{2}[e^{-w}E_1(-w) + e^{w}E_1(w)], \quad (22)$$

while at $\gamma_2^2 = 2$, accordingly, we write the function

$$J_2(c, X) = \frac{C^2(1-c^2)}{2e^2} \times\left\{1 - \frac{w}{2}[e^{w}E_1(w) - e^{-w}E_1(-w)]\right\}. \quad (23)$$

In deriving Eq. (19), we used the approximation of narrow band gaps, $\Lambda \ll \nu_r$, and the condition for the damping due to the inhomogeneities being small, $k_2\gamma_2^2 \ll k_r$. The integral over c was calculated numerically. In the absence of inhomogeneities and when the wave self- damping is neglected, the gap width in the spectrum at $k = k_r$ (corresponding to the distance between the levels of the split spectrum $\nu_+(k_r)$ and $\nu_-(k_r)$) is equal to Λ. In this case, two δ-like peaks separated by the distance Λ will be observed on the dependence $G''(\nu) = \mathrm{Im}G(\nu)$. Recall briefly what happens to the gap in the spectrum and to the form of $G''(\nu)$ when 1D or 3D inhomogeneities appear in the superlattice structure. As the rms fluctuations of the 1D inhomogeneities γ_1 increase, the distance between the levels in the spectrum $\Delta\nu = \nu'_+ - \nu'_-$, where $\nu'_\pm = \mathrm{Re}\nu_\pm(k_r)$, decreases and the gap in the spectrum is closed at some critical value of γ_1. The damping $\nu''_\pm(k) = \mathrm{Im}\nu_\pm(k)$, which as a function of k has a maximum at $k = k_r$ [17], increases simultaneously with γ_1. The peaks on the dependence $G''(\nu)$ decrease and approach each other with increasing γ_1, while their FWHMs increase until these peaks merge into one peak at some γ_1 [18]. The distance between the peaks $\Delta\nu_m \approx \Delta\nu$ at any γ_1. As the rms fluctuations of the 3D inhomogeneities γ_3 increase, $\Delta\nu$ also decreases and, accordingly, $\nu''_\pm$ and Γ increase. However, the decrease in $\Delta\nu$ and $\Delta\nu_m$ for 3D inhomogeneities is slower than that for 1D inhomogeneities and, if the exact formulation is used, leads not to the closure of the gap, but to its exponential smallness [22]. This also applies to the distance between the peaks $\Delta\nu_m$. A characteristic feature of these two cases (1D and 3D inhomogeneities) is that all spectral parameters, the frequencies $\nu'_+(k_r)$ and $\nu'_-(k_r)$, the dampings $\nu''_+(k_r)$ and $\nu''_-(k_r)$, the positions of the maxima of the peaks ν_m^- and ν_m^+, and their FWHMs Γ, are symmetric about the gap center in the approximation under consideration.

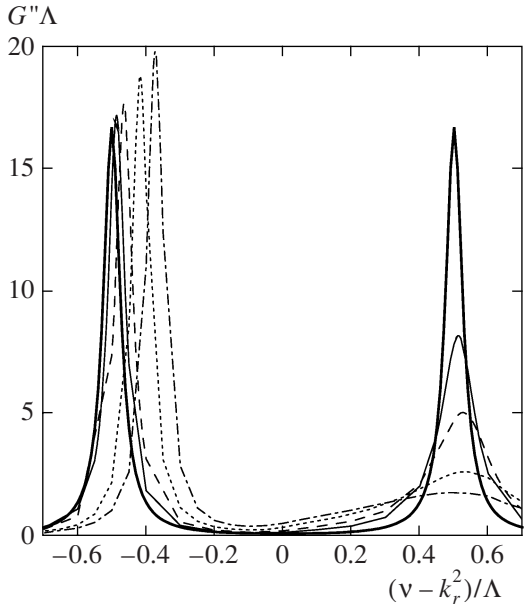

Fig. 2. Imaginary part of the Green function (19) for 2D inhomogeneities at the edge of the first Brillouin zone in a superlattice for $\eta_2 = 4$, $\nu_r/\Lambda = 20$, and various values of γ_2^2: 0 (thick solid curve), 0.2 (thin solid curve), 0.45 (dashed curve), 1.1 (dotted curve), and 1.9 (dash–dotted curve).

The picture for the frequency dependence of the Green function is different when 2D inhomogeneities are present in the superlattice. The results of our calculations for the imaginary part of the Green function (19) are presented in Fig. 2. We see that the left and right peaks of the function G'' differ significantly in behavior as the rms fluctuations of the inhomogeneities γ_2 increase: the left peak shifts to the gap center and slightly increases in amplitude, while the amplitude of the right peak decreases sharply and its FWHM increases. Note that the finite height of the left peak in Fig. 2 and its nonzero FWHM are due to the introduction of a seed damping, $\Gamma_0/\Lambda = 0.03$, in our numerical

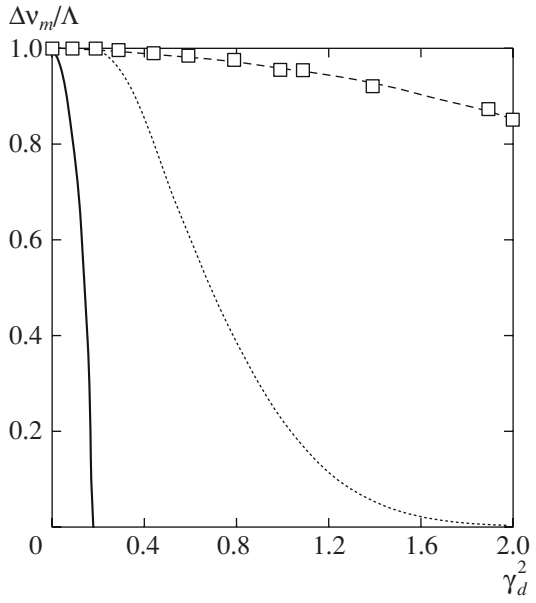

Fig. 3. Distance between the peaks of the imaginary part of the Green function $\Delta\nu_m$ versus γ_2^2 for 1D (solid curve), 2D (squares), and 3D (dotted curve) inhomogeneities; $\eta_d = 4$ ($d = 1, 2, 3$).

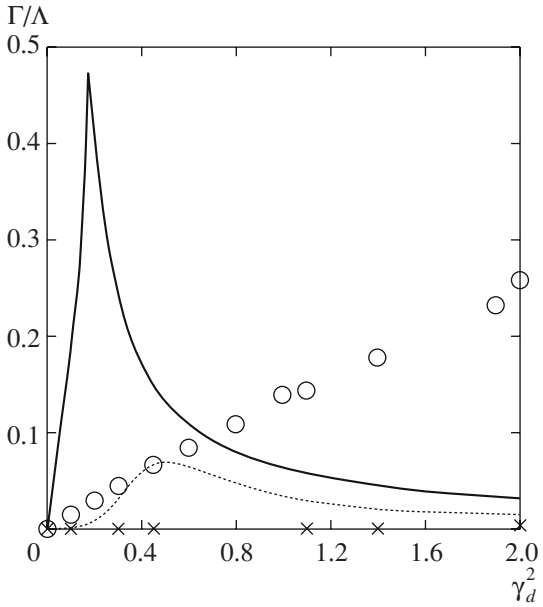

Fig. 4. FWHM Γ of the peaks versus γ_d^2 for 1D (solid curve) and 3D (dotted curve) inhomogeneities. The FWHMs of the left (crosses) and right (circles) peaks for 2D inhomogeneities.

calculations to eliminate the divergences. Thus, the gap closure mechanism for 2D inhomogeneities increasing in intensity turns out to differ from that for 1D or 2D inhomogeneities: the gap disappears due to the reduction in the right peak, while the left peak is retained, as distinct from 1D and 3D inhomogeneities where the gap was closed due to the symmetric approach and broadening of the peaks.

In Fig. 3, the distance between the peaks of the imaginary part of the Green function (19) is plotted against the square of the rms fluctuation of the 2D inhomogeneities γ_2^2 (squares). The previously investigated dependences $\Delta\nu_m(\gamma_1^2)$ and $\Delta\nu_m(\gamma_3^2)$ corresponding to the presence of 1D (solid curve) or 3D (dotted curve) inhomogeneities in the superlattice are also shown here for comparison. We see that the gap in the spectrum is most sensitive to the action of 1D inhomogeneities: the maxima of the Green function merge into a single maximum even at $\gamma_1^2 = \gamma_{1c}^2 = 0.18$ (for $\eta_1 = 4$). Under the action of 3D inhomogeneities, the gap decreases much more slowly: while exponentially decreasing, it virtually disappears at γ_3^2 that are an order of magnitude larger than γ_{1c}^2. The gap in the spectrum and, accordingly, the distance between the maxima m decreases most slowly under the action of 2D inhomogeneities. While decreasing with increasing γ_2^2, $\Delta\nu_m$ decreases only by 15% at $\gamma_2^2 = 2$, while for $\gamma_3^2 = 2$ the gap is already negligible (at $\eta_2 = \eta_3 = 4$).

Figure 4 shows the full widths of the peaks at half maximum of the corresponding peaks of the function $G''(\nu)$. For the previously investigated FWHMs of the peaks under the action of 1D (solid curve) and 3D (dotted curve) inhomogeneities, the peaks are symmetric and the FWHMs of the left and right peaks are equal. The sharp maximum on the solid curve corresponds to the point at which the two peaks merge into one peak at $\gamma_1^2 = \gamma_{1c}^2$. The dependences of the FWHMs of the left and right peaks on γ_2^2 for 2D inhomogeneities investigated here are indicated by the crosses and circles, respectively. When constructing these dependences, we subtracted the seed damping $\Gamma_0/\Lambda = 0.03$ from the calculated FWHMs of the peaks. Therefore, the FWHMs in this figure do not correspond to those in Fig. 2; in particular, the FWHM of the left peak after this operation approximately becomes zero. We see a sharp asymmetry in the FWHMs of the left and right peaks that increases with γ_2^2 almost linearly.

In Fig. 5, the positions of the maxima of the left and right peaks are plotted against the rms fluctuation for 1D, 2D, and 3D inhomogeneities. We see that, in contrast to 1D and 3D inhomogeneities, there is a small asymmetry in the positions of the peaks with respect to the gap center and a shift of the gap center to the higher frequencies for 2D inhomogeneities.

Note that the physical quantities shown in Figs. 3–5 were calculated using expression (20) in Eq. (19) for all values of γ_2^2, except $\gamma_2^2 = 1$ and 2. For the last two val-

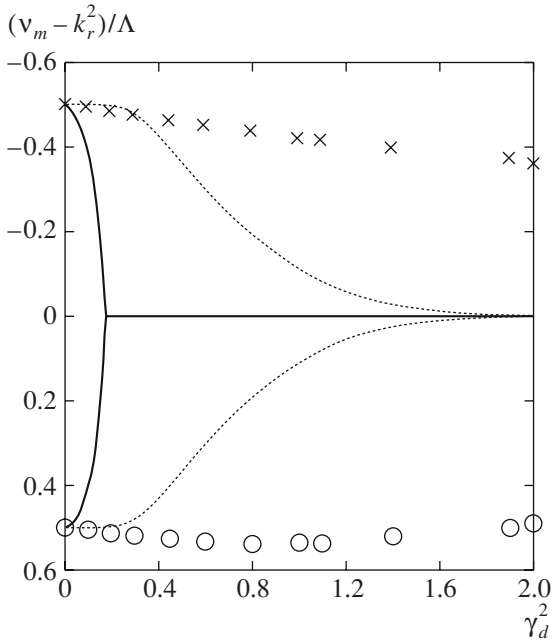

Fig. 5. Positions of the maxima of the peaks versus γ_d^2 for 1D (solid curve) and 3D (dotted curve) inhomogeneities. For 2D inhomogeneities, the crosses and circles correspond to the left and right peaks, respectively.

ues of γ_2^2, we used, respectively, expressions (22) and (23) in Eq. (19). We see that the values of the physical quantities for these selected points fit well into the sequence corresponding to other values of γ_2^2.

4. DISCUSSION

As was shown previously [20–23], the basic characteristics of the wave spectrum are determined mainly by the asymptotics of the correlation functions $K(\mathbf{r})$ for a superlattice when $r \longrightarrow \infty$. Figure 6 shows the shape of the decreasing parts of the correlation functions $K_d(\mathbf{r})$ for 1D, 2D, and 3D inhomogeneities in r_z and $r_\perp$ coordinates for $k_1 = k_2 = k_3$ and $\gamma_1^2 = \gamma_2^2 = \gamma_3^2 = 0.3$. Recall the analysis of the relationship between the characteristics of the wave spectrum and the asymptotics of the correlation functions for superlattices with 1D and 3D inhomogeneities performed in [20]. We consider an initial wave propagating along the z axis perpendicularly to the plane of the superlattice layers. The correlation function of the 1D inhomogeneities with exponential asymptotics for $r_z \longrightarrow \infty$ decreases to zero along the same axis (Fig. 6a). Therefore, the initial wave is intensively scattered by such inhomogeneities, causing a strong damping and a gap closure at low values of γ_1^2 (Figs. 3 and 4, the solid curves). The correlation function for isotropic 3D inhomogeneities decreases equally along all coordinate axes to some asymptote $L = \exp(-3\gamma_3^2)$, but not to zero (Fig. 6c). Thus, the correlation volume above and below this asymptote has finite and infinite correlation lengths, respectively. It is the existence of a correlation volume with an infinite correlation length that leads to a weak wave damping and a slow gap reduction in the spectrum with increasing γ_3^2 (Figs. 3 and 4, the dotted curves).

Let us make a similar comparison of the results obtained in this paper with the correlation function for 2D inhomogeneities. This correlation function decreases as a power law only in the xy coordinate plane (Fig. 6b). Along the propagation axis z of the initial wave, it is constant, i.e., is characterized by an infinite correlation length. Thus, the damping and modification of the dispersion law for the initial wave is determined in this case only by the x and y components of the scattered waves. As a result, the gap in the spectrum decreases with increasing γ_2^2 much more slowly than it does in the cases of 1D and 3D inhomogeneities (Fig. 3, the squares).

It is more convenient to discuss the revealed asymmetry in the FWHMs and amplitudes of the peaks of

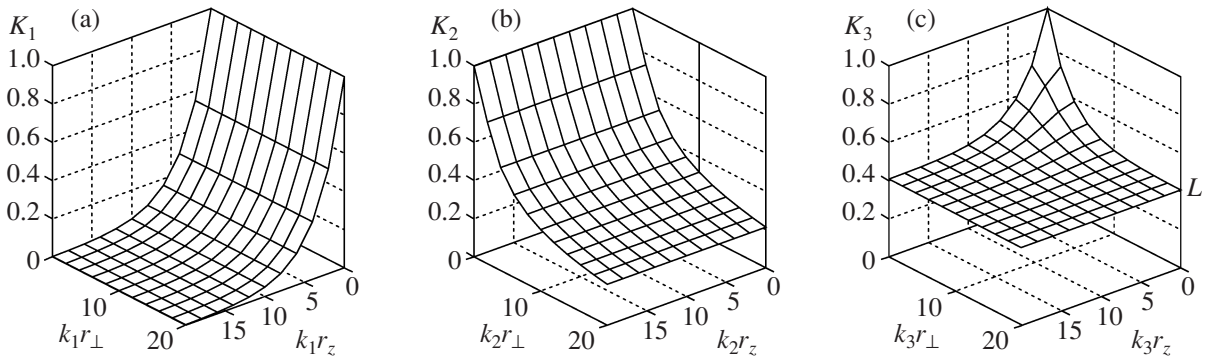

Fig. 6. Decreasing parts of the correlation functions for a superlattice with 1D (a), 2D (b), and 3D (c) inhomogeneities for $\gamma_1^2 = \gamma_2^2 = \gamma_3^2 = 0.3$. The asymptote $L = \exp(-3\gamma_3^2)$ is marked in Fig. 3c.

the Green function arising under the action of 2D inhomogeneities by representing the mass operator of the Green function $M(\nu, k)$ not via the correlation function, as in Eq. (17), but via its Fourier transform, the spectral density $S(\mathbf{k})$. In this case, in Bourret's approximation,

$$M(\nu, \mathbf{k}) = \frac{\Lambda^2}{2}\int\frac{S(\mathbf{k}-\mathbf{k}_s)}{\nu - k_s^2}d\mathbf{k}_s. \quad (24)$$

As is well known, in the processes of wave scattering by inhomogeneities considered here, the energy conservation law must hold for the incident and scattered waves, while the momentum conservation law does not hold. Nevertheless, the constraints that follow from the energy conservation law for the incident and scattered waves and from the dispersion law for the scattered wave are imposed on the absolute value of the momentum. In terms of the frequency of the incident wave ν and the wave vector of the scattered wave k_s, the energy conservation law in an elementary scattering process corresponds to the pole on the real k_s axis in the integrand of Eq. (24) that defines the damping of the incident wave.

Let us consider what constraints the dimension of inhomogeneities imposes on the fulfillment of the energy conservation law. For 3D inhomogeneities, the integration in Eq. (24) is over all directions and magnitudes of the vector $\mathbf{k}_s$; hence, for any frequency ν, the conservation law is $k_s^2 = \nu$. Thus, the damping due to the scattering by inhomogeneities appears at any frequency ν. In the case of 1D inhomogeneities, i.e., random displacements of the interfaces between the superlattice layers, the random phase u_1 depends only on the z coordinate and the spectral density in Eq. (24) takes the form

$$S(\mathbf{k}-\mathbf{k}_s) = S_1(k_z - k_{sz})\delta(k_x - k_{sx})\delta(k_y - k_{sy}). \quad (25)$$

Substituting this expression into (24) and integrating over k_{sx} and k_{sy}, we find that for a wave propagating along the z axis, the energy conservation law in an elementary scattering process takes the form $k_{sz}^2 = \nu$. Only the waves scattered either along the incident wave or in the opposite direction are involved in such processes. However, the integration in (24) is performed over all k_{sz}, which again leads to the possibility of the relation $k_{sz}^2 = \nu$ holding for any frequency ν.

A completely different picture is observed in the presence of 2D inhomogeneities. In this case, for a wave propagating along the z axis, the spectral density is

$$S(\mathbf{k}-\mathbf{k}_1) = \frac{1}{2}S_2(\mathbf{k}_{s\perp}) \times [\delta(k_z - k_{sz} - q) + \delta(k_z - k_{sz} + q)]. \quad (26)$$

Near the right boundary of the Brillouin zone, the second δ function in square brackets may be neglected. This corresponds to the two-wave approximation in which $M(\nu, \mathbf{k})$ after the substitution of Eq. (26) into (24) and the integration over k_{sz} takes the form

$$M(\nu, \mathbf{k}) = \frac{\Lambda^2}{4}\int\frac{S_2(\mathbf{k}_{s\perp})d\mathbf{k}_{s\perp}}{\nu - (k_z - q)^2 - k_{s\perp}^2}, \quad (27)$$

and the energy conservation law is

$$k_{sx}^2 + k_{sy}^2 = \nu - (k_z - q)^2. \quad (28)$$

The presence of the reciprocal superlattice vector $\mathbf{q}$ in the energy relation (28) may suggest that, in this case, we are dealing with one of the types of umklapp processes; the type of the process is difficult to identify accurately, because the momentum conservation law does not hold. It follows from Eq. (28) that the energy conservation law at the boundary of the Brillouin zone for $k_z = k_r = q/2$ takes the form

$$k_{sx}^2 + k_{sy}^2 = \nu - \nu_r, \quad (29)$$

where $\nu_r \equiv k_r^2$ is the frequency corresponding to the center of the band gap in a perfect superlattice. This law can be fulfilled only for frequency $\nu > \nu_r$. For $\nu < \nu_r$, the wave scattering is forbidden. In particular, damping will arise in the region of the right peak of the unperturbed Green function at $\nu = \nu_r + \Lambda/2$ and will be absent in the region of the left peak corresponding to $\nu = \nu_r - \Lambda/2$. Thus, the sharp asymmetry in the dampings for the lower and upper branches of eigenfrequencies and, accordingly, the asymmetry in the FWHMs and amplitudes of the left and right peaks of the Green function in the case of wave scattering by 2D inhomogeneities is a direct consequence of the energy conservation law for the incident and reflected waves.

5. CONCLUSIONS

The following should be noted as a general conclusion to the paper. We found an asymmetry in the amplitudes and FWHMs of the peaks of the Green function at the edges of the band gap in the spectrum of superlattices that arises under the action of 2D inhomogeneities. In our view, this asymmetry can be of interest both in further developing the general theory of the combined effect of periodic and random inhomogeneities of various dimensions on the wave spectrum and in applications. As a result of the asymmetry in the peaks, the gap in the spectrum is closed with increasing rms fluctuations of 2D inhomogeneities not in the traditional way of the approach and symmetric broadening of the peaks of the Green function, characteristic of both 1D and 3D inhomogeneities, but through the broadening and disappearance of only one peak of the Green function corresponding to the high-frequency boundary of the band gap. This effect was shown to be a direct consequence of the energy conservation law for the incident and scattered waves. On the other hand, the asymmetry in the peaks of high-frequency susceptibility can be used in practice to study the inhomogeneities in a

superlattice by spectral methods. An experimental observation of this effect would suggest the presence of precisely 2D inhomogeneities in a superlattice.

Note also the successful (judging by Fig. 1) approximation of the complex formula for the decreasing part of the correlation function for 2D inhomogeneities (Eqs. (6) and (11)) by the simple expression (14), which can also be used in further studies of 2D inhomogeneities.

ACKNOWLEDGMENTS

This work was supported in part by grant no. 3818.2008.3 from the President of Russia in accordance with the program supporting leading scientific schools.

REFERENCES

1. J. B. Shellan, P. Agmon, and P. Yariv, J. Opt. Soc. Am. **68**, 18 (1978).
2. Yu. Ya. Platonov, N. I. Polushkin, N. N. Salashchenko, and A. A. Fraerman, Zh. Tech. Fiz. **57** (11), 2192 (1987) [Sov. Phys. Tech. Phys. **32** (11), 1324 (1987)].
3. J. M. Luck, Phys. Rev. B: Condens. Matter **39**, 5834 (1989).
4. S. Tamura and F. Nori, Phys. Rev. B: Condens. Matter **41**, 7941 (1990).
5. N. Nishiguchi, S. Tamura, and F. Nori, Phys. Rev. B: Condens. Matter **48**, 2515 (1993).
6. G. Pang and F. Pu, Phys. Rev. B: Condens. Matter **38**, 12649 (1988).
7. J. Yang and G. Pang, J. Magn. Magn. Mater. **87**, 157 (1990).
8. D. H. A. L. Anselmo, M. G. Cottam, and E. L. Albuquerque, J. Appl. Phys. **87**, 5774 (1999).
9. L. I. Deych, D. Zaslavsky, and A. A. Lisyansky, Phys. Rev. E: Stat. Phys., Plasmas, Fluids, Relat. Interdiscip. Top. **56**, 4780 (1997).
10. B. A. Van Tiggelen and A. Tip, J. Phys. I **1**, 1145 (1991).
11. A. R. McGurn, K. T. Christensen, F. M. Mueller, and A. A. Maradudin, Phys. Rev. B: Condens. Matter **47**, 13120 (1993).
12. M. M. Sigalas, C. M. Soukoulis, C.-T. Chan, and D. Turner, Phys. Rev. B: Condens. Matter **53**, 8340 (1996).
13. V. A. Ignatchenko, R. S. Iskhakov, and Yu. I. Mankov, J. Magn. Magn. Mater. **140–144**, 1947 (1995).
14. A. G. Fokin and T. D. Shermergor, Zh. Éksp. Teor. Fiz. **107** (1), 111 (1995) [Phys.—Usp. **80** (1), 58 (1995)].
15. A. V. Belinskii, Usp. Fiz. Nauk **165** (6), 691 (1995) [Phys.—Usp. **38** (6), 623 (1995)].
16. B. Kaelin and L. R. Johnson, J. Appl. Phys. **84** (Part I), 5451; (Part II), 5458 (1998).
17. V. A. Ignatchenko and Yu. I. Mankov, Phys. Rev. B: Condens. Matter **56**, 194 (1997).
18. V. A. Ignatchenko, Yu. I. Mankov, and A. V. Pozdnyakov, Zh. Éksp. Teor. Fiz. **116** (4), 1335 (1999) [JETP **89** (4), 717 (1999)].
19. V. A. Ignatchenko, A. A. Maradudin, and A. V. Pozdnyakov, Phys. Met. Metallogr. **91** (Suppl. 1), S69 (2001).
20. V. A. Ignatchenko, Yu. I. Mankov, and A. A. Maradudin, Phys. Rev. B: Condens. Matter **68**, 024209 (2003).
21. V. A. Ignatchenko and Yu. I. Mankov, Fiz. Tverd. Tela (St. Petersburg) **47** (3), 565 (2005) [Phys. Solid State **47** (3), 587 (2005)].
22. V. A. Ignatchenko and Yu. I. Mankov, Zh. Eksp. Teor. Fiz. **129** (4), 710 (2006) [JETP **102** (4), 625 (2006)].
23. V. A. Ignatchenko and Yu. I. Mankov, Phys. Rev. B: Condens. Matter **75**, 235422 (2007).
24. A. N. Malakhov, Zh. Eksp. Teor. Fiz. **30**, 884 (1956) [Sov. Phys. JETP **3**, 701 (1956)].
25. S. M. Rytov, Y. A. Kravtsov, and V. I. Tatarskii, *Principles of Statistical Radiophysics* (Nauka, Moscow, 1976; Springer, Berlin, 1987–1989), Part I.
26. R. C. Bourret, Nuovo Cimento **26**, 1 (1962); Can. J. Phys. **40**, 782 (1962).

Translated by V. Astakhov